

Dancing vortices in a driven nematic liquid crystal cell: Theory and experimentM. G. Clerc, M. Ferré, R. Gajardo-Pizarro , and V. Zambra *Departamento de Física and Millennium Institute for Research in Optics, FCFM, Universidad de Chile, Casilla 487-3, Santiago, Chile*

(Received 3 February 2022; accepted 30 June 2022; published 19 July 2022)

The interaction of light beams with helical defects in optical materials generates optical vortices. Understanding and manipulating the dynamics of helical defects allows for the creation of versatile sources of optical vortex beams. Using a magnetic ring on a nematic liquid crystal cell, we trapped helical defects identified as matter vortices. We observe oscillatory rotating and beating matter vortices by applying a low-frequency voltage. Experimentally, we determine the region of parameters where these vortices are observed. The amplitude of oscillatory rotating vortices decays with the inverse of the voltage frequency. We propose an adequate amplitude equation, which allows us to describe the vortex dynamics; theoretical findings have a qualitative agreement with the experimental observations.

DOI: [10.1103/PhysRevE.106.L012201](https://doi.org/10.1103/PhysRevE.106.L012201)

Extended systems out of equilibrium can present particle-like solutions when they are locally disturbed [1–7]. Classic examples are the solitary waves observed in coupled oscillators, fluids, magnetic media, chemical reactions, liquid crystals, and fiber optics, to mention a few. These solutions are characterized by being localized and well-defined shapes (typically with a bell profile), usually described by their position, width, height, and charge, depending on the physics of the system under study [1–7]. Likewise, these particles interact with each other [8–13]. In addition, these solutions can also be destroyed by employing local disturbances. This previous scenario changes drastically when considering vortex or phase singularity solutions. Vortices are particlelike solutions with topological features [4]. Most precisely, vortices are pointlike singularities in complex fields, which locally break rotation symmetry [14]. These properties are responsible for the stability of the vortices. The position of the vortices is characterized by having zero magnitude of the amplitude, in which the phase field is singular and has a spiral structure. The number of phase jumps accounts for the topological charge, while the direction of rotation determines their sign. Because of the conservation of the global topological charge, vortices are created and annihilated by pairs between opposite charges [8–12]. When considering inhomogeneities, the previous dynamical behavior changes can attract and trap vortices [15]. Likewise, inhomogeneous anchoring allows for attracting and trapping defects and creating vortex lattices [16]. Similar spontaneous stable vortex lattices can be achieved by employing thermal gradients [17], doping with ionic impurity [18], or applying low-frequency voltages [18,19]. Optical vortices have drawn attention for their different applications [20], such as optical tweezers [21–23], quantum computation [24], enhancement of astronomical images [25], and data transmission [26]. An efficient strategy to generate optical vortices is through the interaction of a light beam with phase singularity in liquid crystals through q -plates [27], cells with photosensitive walls [13], or cells with a combination of magnetic rings and electric

fields [28]. These methods are characterized by the fixation of umbilical defects induced by boundary conditions, electric and magnetic, or electromagnetic fields. Understanding and manipulating the dynamics of point defects in liquid crystals allow for the creation of new and versatile sources of optical vortices.

This Letter aims to understand and characterize the emergence of oscillatory rotating and beating vortices in liquid crystals. Based on a nematic liquid crystal cell with a homeotropic anchoring and negative dielectric anisotropy under the influence of an oscillatory electric field, and the effect of a magnetic ring oscillatory rotating matter, vortices with a positive charge are observed, called *rotating vortices* (cf. Fig. 1). Vortices of negative charge do not rotate, but their core is characterized by increasing and decreasing periodically, referred to as *beating vortices*. We have termed these vortices as dancing. Different dynamical behaviors are observed when the voltage frequency is changed. Experimentally, we characterize the region of parameters where the dancing vortices are observed. The amplitude of oscillatory rotating vortices decays with the inverse of the voltage frequency. Theoretically, we propose a modification of an amplitude equation used to describe liquid crystal cells, in the limit of high frequencies of voltage, close to the reorientational transition, which presents dancing vortices. The theoretical model exhibits similar behaviors to those observed experimentally.

Experimental setup. To study the vortex features, we use a magnetic trap, composed of a nematic liquid crystal cell under the influence of an electric field and a magnetic ring. Figure 1(a) depicts a schematic representation of the experimental setup. We consider a cell composed of two thin glass layers separated by a thickness of $d = 75 \mu\text{m}$, which is chemically treated on its internal walls to have a homogeneous homeotropic anchoring and with transparent electrodes included (indium tin oxide with a thickness of $0.08 \mu\text{m}$). By capillarity the cell is filled with a nematic liquid crystal LC-BYVA (Instec) with negative dielectric anisotropy $\epsilon_a =$

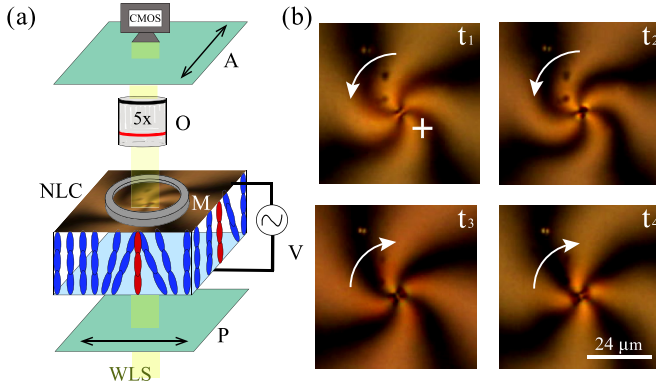


FIG. 1. Dancing vortex. (a) Schematic representation of the experimental setup. A nematic liquid crystal cell (NLC) is under the effect of a magnet ring (M) and the oscillatory electric field generated by a voltage $V = V_0 \sin(\omega t)$, where V_0 and ω are the intensity and frequency of the applied voltage. P and A are crossed and linear polarizers. The sample is illuminated by a white light source (WLS). O is an objective, and CMOS is a camera to monitor the liquid crystal cell. The color rods account for a schematic representation of the average molecular orientation of the liquid crystal cell. All the experiments were conducted at a $T = 21^\circ\text{C}$ temperature. (b) Time sequence of snapshots of a positive umbilical defect in a nematic liquid crystal cell ($t_1 = 0$ s, $t_2 = 0.13$ s, $t_3 = 0.4$ s, $t_4 = 0.47$ s).

-4.89 , birefringence $\Delta n = n_e - n_o = 0.1$, rotation viscosity $\gamma = 204$ mPa s, splay and bend elastic constants, respectively, $K_1 = 17.65$ pN and $K_3 = 21.39$ pN, and negative magnetic anisotropy χ_a (not yet measured). A neodymium magnetic ring of 3200 G with a rectangular transversal section, outer radius $R_{\text{out}} = 7$ mm, internal radius $R_{\text{in}} = 2$ mm, and thickness of $h = 5$ mm is put onto the top of the nematic liquid crystal cell (cf. Fig. 1). The cell with the magnetic ring is introduced in an Olympus Bx51 microscope and it is sandwiched between two linear cross polarizers. The polarizers are, respectively, represented by P and A [see Fig. 1(a)]. A sinusoidal voltage $V = V_0 \sin(\omega t)$ of intensity V_0 ranging between 15 and 45 V_{pp}, above of the reorientational transition [29,30], the Fréedericksz voltage $V_{\text{FT}} = 6.57$ V_{pp}. The frequency ω is a control parameter in the present study, which varies between kHz and fractions of Hz. The system is illuminated by a white light (halogen lamp). The temporal evolution of the liquid crystal cell under the simultaneous effects of the electric and magnetic field is monitored by a complementary metal-oxide-semiconductor (CMOS) camera (Thorlabs DCC1645C), which allows us to observe the central zone of the magnetic ring. All experimental analyses were conducted at a room temperature of 21°C .

Experimental results. When a nematic liquid crystal cell with a negative dielectric constant and homeotropic anchoring is under the influence of a sufficiently large vertical voltage, it presents umbilical defects [29,30]. To avoid charge accumulation, called *capacitive effects*, onto the liquid crystal cells, an alternating voltage with a frequency of the order of kHz is usually applied. This type of voltage originates a vertical effective constant electric field without a privileged direction. In this region of parameters, cells are characterized by presenting two types of stationary vortices, called *standard vortices*,

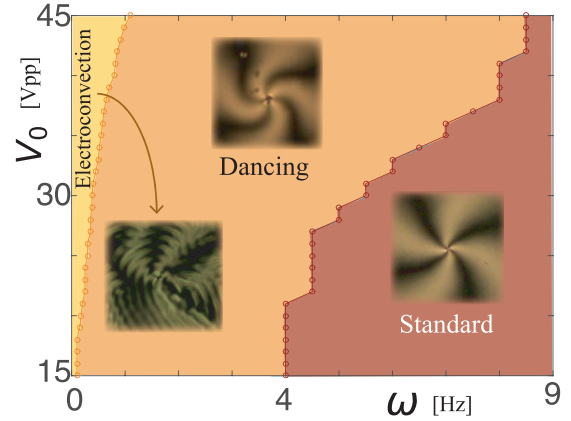


FIG. 2. Vortex phase diagram as a function of the frequency ω and intensity V_0 of the voltage. In the brown, orange, and yellow regions, standard and dancing vortices with and without electroconvection are observed, respectively. Insets show typical snapshots of the observed vortices. The circles account for the results obtained experimentally and the lines that connect them have been interpolated to separate the different regions.

with positive and negative topological charge [29,30]. These vortices repel (attract) if they have the same (opposite) topological charge. Indeed, as a consequence of this interaction, the observation and characterization of vortices is a transient phenomenon, because the system minimizes its free energy.

A simple and efficient manner to study vortices is to consider vortex traps by employing a magnetic ring [28]. A positive vortex is positioned at the ring center, and a pair of vortices of opposite charge on the outside, called a *vortex triplet*. For frequencies of applied voltage that vary in the range of tens to kHz, only standard vortices are observed, as illustrated in the phase diagram shown in Fig. 2. By decreasing the frequency at a given voltage intensity, we observe oscillatory rotating and beating matter vortices. Positively (negatively) charged vortices are characterized by oscillatory rotating arms (core beating)—see Video 1 in the Supplemental Material [31]. Figure 2 shows the phase diagram as a function of the strength intensity V_0 and frequency ω . The experimental curves that separate the different regions are determined when we detect that the arms of the vortices oscillate or electroconvection patterns appear. At lower-frequency values, we observe the emergence of electroconvection, which is characterized by the appearance of oscillatory patterns (stripes and squares depending on the forcing parameters) as a result of the movement of charges and coupling with the fluid dynamics of the liquid crystal [30]. Note that vortices are persistent under the presence of electroconvection.

To characterize the dynamics of the dancing vortices, we have monitored the dynamics of the vortex arms (dark curves emerging from the vortex position when cross-linear polarizers are considered). By fixing a reference axis, we measure the temporal evolution of the angle of the vortex arms, considering a length segment of the order of $20 \mu\text{m}$. Figure 3 summarizes the temporal evolution of the angle of the vortex arms. From this chart, we can infer that the movement of vortex arms has a periodic nature and does not perform a harmonic movement. The fundamental frequency of oscillation

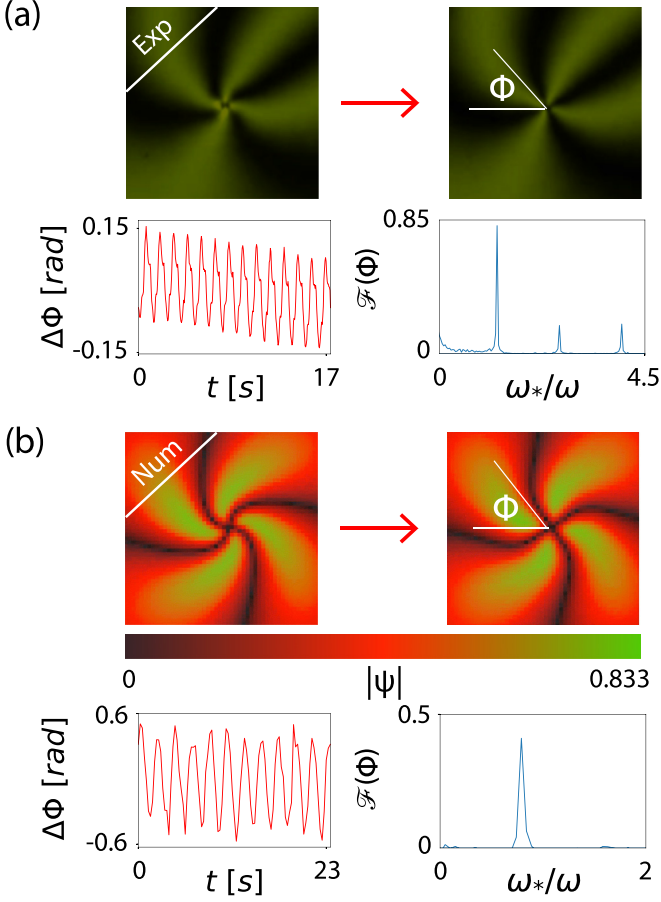


FIG. 3. Rotating vortices, and oscillatory dynamics of positively charged vortices. (a) Experimental and (b) numerical characterization of the oscillation of the vortices following the evolution of the vortex arms, and their respective Fourier transform $\mathcal{F}[\Delta\phi](\omega_*)$ with respect to the voltage frequency ω . The symbol $\psi = \text{Re}(A)\text{Im}(A)$ accounts for the polarized field, with A the order parameter of Eq. (3).

is equal to the frequency of the voltage ω . In the temporal evolution of the angle, there is a tendency for the reference angle to decay to saturation, a consequence of the vortex moving slowly towards the center of the magnet ring. When changing the frequency ω , we observe that the amplitude $\Delta\Phi$ of the rotational oscillation of the positive charges and the amplitude ΔC of the beat of the nucleus of the vortices with negative charges decrease with the inverse of the frequency ω , that is, $\Delta\Phi \propto 1/\omega$ and $\Delta C \propto 1/\omega$. Figure 4 summarizes these dynamical behaviors. As follows, we provide an explanation for the origin of these experimental observations.

Theoretical description. Nematic liquid crystals are characterized by the present molecular orientation, but not a positional order [29,30]. Considering a fixed temperature, this molecular orientation is described by the vector field $\vec{n}(\vec{r}, t)$, usually termed as the director [29,30]. When one considers a nematic liquid crystal cell with homeotropic anchoring, as a result of an elastic interaction, the molecules are oriented orthogonal to the wall cells, resulting in a homeotropic state $\vec{n} = \hat{z}$, where \hat{z} accounts for a unitary vector orthogonal to the wall cells. In the case where the liquid crystal has a negative anisotropic dielectric constant, when applying a sufficiently

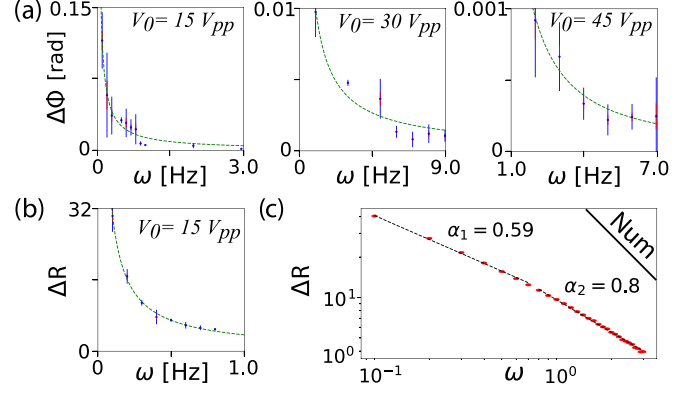


FIG. 4. Experimental amplitudes of oscillation of the phase $\Delta\phi$ and magnitude ΔR of the vortex as a function of the frequency of the voltage ω . (a) The amplitude of oscillation of the vortex phase as a function of frequency for different applied voltages (V_{pp} refers to peak-to-peak voltage). (b) The amplitude of oscillation of the vortex magnitude as a function of frequency. Points and error bars are the results obtained experimentally. The dashed lines are the fits obtained using the law of inverse frequency. (c) The amplitude of oscillation of the magnitude of the vortex as a function of the frequency obtained numerically for the model Eq. (3) with $\mu(r) = \alpha + \alpha_0 \exp[-r^2/(2\sigma^2)] + \mu_1 \cos(\omega t)$, $f(r) = \epsilon_r r \exp[-r^2/(2\sigma^2)]$, $\delta = 0$, $\delta_0 = 0.2$, $K = 0$, $K_0 = 0.2$, $\alpha = -0.2$, $\alpha_0 = 1.65$, $\epsilon_r = 0.001$, $\sigma = 40$, and $\mu_1 = 0$.

large vertical electric field, molecules become misaligned with the direction of the electric field, generating a *reorientation instability* [29,30,32]. This instability is known as the Fréedericksz transition [32]. At a large frequency limit of the voltage, near the orientational instability of the molecules, the director can be approached by [33]

$$\vec{n}(r, \theta, z) \approx \begin{pmatrix} u(r, \theta, t) \sin(\frac{\pi z}{d}) \\ w(r, \theta, t) \sin(\frac{\pi z}{d}) \\ 1 - \frac{(u^2 + w^2)}{2} \sin^2(\frac{\pi z}{d}) \end{pmatrix}, \quad (1)$$

where d is the thickness of the cell and $\{r, \theta, z\}$ are the cylindrical coordinates. Introducing the complex order parameter $A = u + iw$ in the director equation close to the reorientational instability and including the effect of a magnetic ring after straightforward calculations, the dimensionless amplitude equation of the order parameter reads [28,34]

$$\partial_t A = \mu_0(r)A - A|A|^2 + K\nabla_{\perp}^2 A + \delta\partial_{\eta,\eta} \bar{A} + f(r)e^{i\theta}, \quad (2)$$

where $\mu_0(r)$ is the bifurcation parameter which has a bell shape, $\partial_{\eta} \equiv \partial_x + i\partial_y$ (Wirtinger derivative), K and δ account, respectively, for the elastic isotropy and anisotropy, and $f(r)$ stands for the magnetic forcing that near the center of the ring has the shape of the spatial variation of the bifurcation parameter (for its explicit expression, see Ref. [34]). A detailed derivation of the amplitude equation and relation of the parameters with the physical one is available in Refs. [28,33,34]. The amplitude Eq. (2) has been used to explain several phenomena such as vortex induction via an anisotropy stabilized light-matter interaction [33,35], symmetry breaking of nematic umbilical defects [36], light-matter interaction inducing a shadow vortex [37], the origin of the optical vortex lattices [38], and the magnetic field-induced vortex triplet and vortex

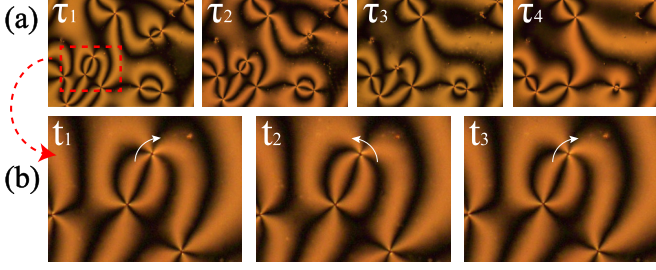


FIG. 5. Dynamics of dancing vortices in a liquid crystal cell under the effect of low-frequency voltage without a magnetic ring. (a) Time sequence of snapshots ($\tau_1 = 0$ s, $\tau_2 = 24.3$ s, $\tau_3 = 48.6$ s, $\tau_4 = 72.9$ s). (b) Time sequence magnification of snapshots ($t_1 = 8.1$ s, $t_2 = 8.5$ s, $t_3 = 8.9$ s). For more details, see Video 3 in the Supplemental Material [31].

lattice [28]. In particular, model (2) accounts for the features and dynamics of umbilical defects in nematic liquid crystals under the effect of high-frequency electric fields, i.e., standard vortices.

When the voltage frequency is decreased, the dynamics of the vortices are coupled to charge movements and fluids, which makes the liquid crystal theory and dynamics of paramount complexity. To describe the dynamics observed by vortices, we phenomenologically promote some parameters to oscillatory ones and the modified model (2) reads

$$\partial_t A = \mu(r, t)A - A|A|^2 + \tilde{K}\nabla_{\perp}^2 A + \tilde{\delta}\partial_{\eta, \eta}\bar{A} + f(r)e^{i\theta}, \quad (3)$$

where $\mu(r, t) = \mu_0(r) + \mu_1 \cos(\omega t)$, $\tilde{K}(t) = K + iK_0 \cos(\omega t)$, and $\tilde{\delta}(t) = \delta + \delta_0 \cos(\omega t)$ are parametrically driven parameters. μ_1 , K_0 , and δ_0 account for a parametric forcing of the bifurcation parameter, the spatial phase modulation, and the anisotropic elastic coupling, respectively. μ_1 is responsible for the oscillation in the hue observed for the extended homogeneous state (see Video 1 in the Supplemental Material [31]). Numerical simulations of the phenomenological model (3) show dancing vortices. Figure 3(b) shows a typical dancing vortex of model (3). The vortex arms are characterized by exhibiting a more harmonic oscillation than that observed experimentally [see Fig. 3(b) and Video 2 in the Supplemental Material [31]]. Likewise, when one does not consider the forcing term ($f = 0$), the simulations show dancing vortices and the interaction between them, similar to those observed experimentally when the magnetic ring is not considered (see Fig. 5).

To explain the origin of the oscillatory behavior of the phase and amplitude of the vortex with a positive charge, we use the perturbative method at the high-frequency limit, $\omega \rightarrow \infty$. At this limit, using the time averaging method [39], one can reobtain the model Eq. (2) from Eq. (3). Model Eq. (2) has unknown vortex solutions analytically, and only for negative bifurcation parameters, it has analytically known solutions, called the *Rayleigh vortex* [38]. To reveal the dynamics of the vortices in the presence of the oscillatory terms, we consider the ansatz

$$A = [R(r) + \Delta R(r, t)]e^{i[\theta + \Delta\phi(r, t)]}, \quad (4)$$

where $R(r)e^{i\theta}$ is the vortex solution of model Eq. (2), i.e., it is a solution of Eq. (3) with $K_0 = \delta_0 = \mu_1 = 0$. $\Delta R(r, t)$ and

$\Delta\phi(r, t)$ are small correction functions of the magnitude and phase of the amplitude A [$\Delta R(r, t) \ll 1$ and $\Delta\phi(r, t) \ll 1$]. Introducing the ansatz (4) in model Eq. (3), after straightforward calculations at the dominant order, we obtain ($\omega \gg 1$)

$$\Delta\phi(r, t) \approx \frac{k_0}{\omega} \sin(\omega t) \left[\partial_{rr} R + \frac{\partial_r R}{r} - \frac{R}{r^2} \right], \quad (5)$$

$$\Delta R(r, t) \approx \frac{\delta_0}{\omega} \sin(\omega t) \left[\partial_{rr} R + \frac{\partial_r R}{r} - \frac{R}{r^2} \right]. \quad (6)$$

The corrections to the previous expressions are of the ω^{-2} order. From expression (5), we can infer that the vortex phase has an oscillatory rotation that depends on the inverse of the voltage frequency, which agrees with the experimental observations [see Fig. 4(a)]. Numerical simulations of model Eq. (3) show that the amplitude of the oscillation of the phase exhibits different behaviors. For large frequencies, the model Eq. (3) presents a power law of form $\Delta\phi(r, t) \propto \omega^{-n}$, $n \approx 0.8$, and for smaller frequencies, this law is modified to $\Delta\phi(r, t) \propto \omega^{-n}$ and $n \approx 0.6$. The origin of the discrepancy between numerical simulations and formula (5) is related to the role of the high-order corrections. Hence, the experimental and numerical findings have qualitative agreements. Likewise, we find a qualitative agreement for the dependence of the magnitude of the amplitude as a function of the frequency of the voltage [see Fig. 4(b)]. From formulas (5) and (6), we can infer that the oscillatory corrections are only relevant near the vortex core since, far from it, these corrections are negligible. This is consistent with the experimental observations, where only the vortex rotates or oscillates around the vortex core (see videos in the Supplemental Material [31]). Note that if one incorporates imaginary coefficients in the linear or cubic terms of the amplitude equation, which would give rise to phase modulations, they will generate a rigid rotation of the vortex, which is not observed experimentally. Due to the more complex structure of the negative charge, a similar analytical study showing its respiratory behavior is still an open problem.

Conclusions. Liquid crystals are dielectric media with weak and anisotropic conductivity [30], which activates the movement of electric charges and fluid at low frequencies (fractions of Hz). These effects change the dynamics of liquid crystals at high frequencies. We have studied the dynamics of vortices when applying a low-frequency voltage and a magnetic field generated by a magnetic ring. We observe that umbilical defects become oscillating, rotating, and beating. The amplitude of the oscillating rotating vortices decays with the inverse of the voltage frequency. Experimentally, we determine the parameter region where the dancing vortices are observed. A suitable phenomenological amplitude equation allows for describing the dancing vortices, which present behaviors similar to those observed experimentally. A more appropriate theoretical description of the system under study should consider the dynamics of molecular reorientation, fluid motion, and charge movements (Ericksen-Leslie theory coupled with Maxwell's equations). One could derive a minimal model from this description. However, this is a thorny task.

The magnetic ring is employed to trap a vortex in a given position and study its properties. When one does not consider the ring magnet and applies a low-frequency voltage, we

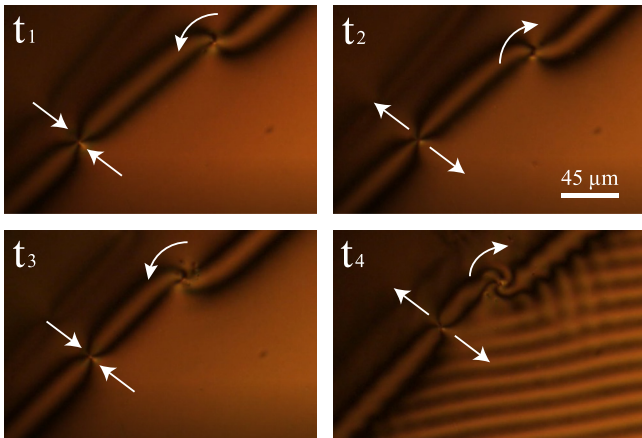


FIG. 6. Dancing vortex interaction. Time sequence of snapshots ($t_1 = 0$ s, $t_2 = 240$ s, $t_3 = 480$ s, $t_4 = 720$ s). The arrows account for the dynamics of the vortices (rotation and beats).

observe the emergence of dancing vortices, which are later annihilated by pairs (oscillatory and beating). Hence, the system converges to a transversal homogeneous orientation state

without vortices. Figure 5 and Video 3 in the Supplemental Material [31] depict the observed dynamics of dancing vortices in the liquid crystal cell under the effect of low-frequency voltage. Therefore, the magnetic field does not significantly modify the dynamics of the dancing vortices.

The interaction of vortices for high frequency has been carefully studied [13]; establishing an interaction depends on the inverse of the distance with a mobility that is a function of the speed of vortices. The interaction at low frequencies is completely modified by the oscillations (see Fig. 6), which slow down the attraction of the vortices. The study of interactions is a problem in progress. Our observations open different avenues for understanding out-of-equilibrium topological defects and their applications. In particular, the dynamics of the vortices in the electroconvection regime show the robustness of the vortices in complex, even turbulent, media. Their understanding can play an essential role in communication in free space.

Acknowledgments. The authors thank Vincent Odent for fruitful discussions and preliminary observations. The authors acknowledge the financial support of FONDECYT Project No. 1210353 and ANID-Millennium Science Initiative Program ICN17_012 (MIRO).

-
- [1] M. C. Cross and P. C. Hohenberg, Pattern formation outside of equilibrium, *Rev. Mod. Phys.* **65**, 851 (1993).
- [2] A. C. Newell, *Solitons in Mathematics and Physics* (Society for Industrial and Applied Mathematics, Philadelphia, 1985).
- [3] M. Remoissenet, *Waves Called Solitons: Concepts and Experiments* (Springer, Heidelberg, 1993).
- [4] L. M. Pismen, *Patterns and Interfaces in Dissipative Dynamics* (Springer, Berlin, 2006).
- [5] *Dissipative Solitons: From Optics to Biology and Medicine*, edited by N. Akhmediev and A. Ankiewicz, Lecture Notes in Physics Vol. 751 (Springer, Heidelberg, 2008).
- [6] H. G. Purwins, H. U. Bodeker, and S. Amiranashvili, Dissipative solitons, *Adv. Phys.* **59**, 485 (2010).
- [7] O. Descalzi, M. G. Clerc, S. Residori, and G. Assanto, *Localized States in Physics: Solitons and Patterns* (Springer, Berlin, 2011).
- [8] T. Nagaya, H. Hotta, H. Orihara, and Y. Ishibashi, Observation of annihilation process of disclinations emerging from bubble domain, *J. Phys. Soc. Jpn.* **60**, 1572 (1991).
- [9] A. N. Pargellis, P. Finn, J. W. Goodby, P. Panizza, B. Yurke, and P. E. Cladis, Defect dynamics and coarsening dynamics in smectic-C films, *Phys. Rev. A* **46**, 7765 (1992).
- [10] P. Tóth, N. Éber, T. M. Bock, A. Buka, and L. Kramer, Dynamics of defects in electroconvection patterns, *Europhys. Lett.* **57**, 824 (2002).
- [11] I. Dierking, O. Marshall, J. Wright, and N. Bulleid, Annihilation dynamics of umbilical defects in nematic liquid crystals under applied electric fields, *Phys. Rev. E* **71**, 061709 (2005).
- [12] M. G. Clerc, S. Coulibaly, N. Mujica, R. Navarro, and T. Sauma, Soliton pair interaction law in parametrically driven Newtonian fluid, *Philos. Trans. R. Soc. A* **367**, 3213 (2009).
- [13] R. Barboza, T. Sauma, U. Bortolozzo, G. Assanto, M. G. Clerc, and S. Residori, Characterization of vortex pair interaction law and nonlinear, *New J. Phys.* **15**, 013028 (2013).
- [14] L. M. Pismen, *Vortices in Nonlinear Fields* (Oxford Science, New York, 1999).
- [15] M. Kim and F. Serra, Tunable dynamic topological defect pattern formation in nematic liquid crystals, *Adv. Opt. Mater.* **8**, 1900991 (2020).
- [16] B. S. Murray, R. A. Pelcovits, and C. Rosenblatt, Creating arbitrary arrays of two-dimensional topological defects, *Phys. Rev. E* **90**, 052501 (2014).
- [17] P. Pieranski, E. Dubois-Violette, and E. Guyon, Heat Convection in Liquid Crystals Heated from Above, *Phys. Rev. Lett.* **30**, 736 (1973).
- [18] Y. Sasaki, V. S. R. Jampani, C. Tanaka, N. Sakurai, S. Sakane, K. V. Le, F. Araoka, and H. Orihara, Large-scale self-organization of reconfigurable topological defect networks in nematic liquid crystals, *Nat. Commun.* **7**, 13238 (2016).
- [19] M. G. Clerc, M. Kowalczyk, and V. Zambra, Topological transitions in an oscillatory driven liquid crystal cell, *Sci. Rep.* **10**, 19324 (2020).
- [20] A. S. Desyatnikov, Y. S. Kivshar, and L. Torner, in *Progress in Optics*, edited by E. Wolf (Elsevier, Amsterdam, 2005), Vol. 47, p. 291.
- [21] D. G. Grier, A revolution in optical manipulation, *Nature (London)* **424**, 810 (2003).
- [22] V. G. Shvedov, A. V. Rode, Y. V. Izdebskaya, A. S. Desyatnikov, W. Krolikowski, and Y. S. Kivshar, Giant Optical Manipulation, *Phys. Rev. Lett.* **105**, 118103 (2010).
- [23] M. Padgett and R. Bowman, Tweezers with a twist, *Nat. Photonics* **5**, 343 (2011).
- [24] H. H. Arnaut and G. A. Barbosa, Orbital and Intrinsic Angular Momentum of Single Photons and Entangled Pairs of Photons Generated by Parametric Down-Conversion, *Phys. Rev. Lett.* **85**, 286 (2000).

- [25] F. Tamburini, G. Anzolin, G. Umbriaco, A. Bianchini, and C. Barbieri, Overcoming the Rayleigh Criterion Limit with Optical Vortices, *Phys. Rev. Lett.* **97**, 163903 (2006).
- [26] J. Wang, J.-Y. Yang, I. M. Fazal, N. Ahmed, Y. Yan, H. Huang, Y. Ren, Y. Yue, S. Dolinar, M. Tur, and A. E. Willner, Terabit free-space data transmission employing orbital angular momentum multiplexing, *Nat. Photonics* **6**, 488 (2012).
- [27] L. Marrucci, C. Manzo, and D. Paparo, Optical Spin-to-Orbital Angular Momentum Conversion in Inhomogeneous Anisotropic Media, *Phys. Rev. Lett.* **96**, 163905 (2006).
- [28] E. Calisto, M. G. Clerc, and V. Zambra, Magnetic field-induced vortex triplet and vortex lattice in a liquid crystal cell, *Phys. Rev. Research* **2**, 042026(R) (2020).
- [29] S. Chandrasekhar, *Liquid Crystals* (Cambridge University Press, Cambridge, UK, 1992).
- [30] P. G. de Gennes and J. Prost, *The Physics of Liquid Crystals*, 2nd ed. (Oxford Science/Clarendon, Oxford, UK, 1993).
- [31] See Supplemental Material at <http://link.aps.org/supplemental/10.1103/PhysRevE.106.L012201> for videos 1 and 2, which show an experimental movie of the dynamics of two oscillatory vortices with different charges and a numerical simulation of the dancing vortex of model Eq. (3), respectively. Video 3 shows the dynamics of dancing vortices in a liquid crystal cell under the effect of low-frequency voltage without a magnetic ring.
- [32] V. Fréedericksz and V. Zolina, Forces causing the orientation of an anisotropic liquid, *Trans. Faraday Soc.* **29**, 919 (1933).
- [33] R. Barboza, U. Bortolozzo, M. G. Clerc, S. Residori, and E. Vidal-Henriquez, Optical vortex induction via light-matter interaction in liquid-crystal media, *Adv. Opt. Photon.* **7**, 635 (2015).
- [34] E. Calisto, Vortices induced by topological forcing in nematic liquid crystal layers, M.Sc. dissertation, University of Chile, <https://repositorio.uchile.cl/handle/2250/174821>.
- [35] R. Barboza, U. Bortolozzo, G. Assanto, E. Vidal-Henriquez, M. G. Clerc, and S. Residori, Vortex Induction via Anisotropy Stabilized Light-Matter Interaction, *Phys. Rev. Lett.* **109**, 143901 (2012).
- [36] M. G. Clerc, E. Vidal-Henriquez, J. D. Davila, and M. Kowalczyk, Symmetry breaking of nematic umbilical defects through an amplitude equation, *Phys. Rev. E* **90**, 012507 (2014).
- [37] R. Barboza, U. Bortolozzo, M. G. Clerc, J. D. Davila, M. Kowalczyk, S. Residori, and E. Vidal-Henriquez, Light-matter interaction induces a shadow vortex, *Phys. Rev. E* **93**, 050201(R) (2016).
- [38] E. Calisto, M. G. Clerc, M. Kowalczyk, and P. Smyrnelis, the origin of the optical vortex lattices in a nematic liquid crystal light valve, *Opt. Lett.* **44**, 2947 (2019).
- [39] N. N. Bogoliubov and Y. A. Mitropolski, *Asymptotic Methods in the Theory of Non-Linear Oscillations* (Gordon and Breach, New York, 1961).